Non-classical photon streams using rephased amplified spontaneous emission

Patrick M. Ledingham, William R. Naylor, and Jevon J. Longdell*

Jack Dodd Centre for Photonics and Ultra-Cold Atoms,
Department of Physics, University of Otago, Dunedin, New Zealand.

Sarah E. Beavan, and Matthew J. Sellars

Laser Physics Centre, RSPhysSE, Australian National University, Canberra, ACT 0200, Australia

(Dated: November 20, 2009)

We present a fully quantum mechanical treatment of optically rephased photon echoes. These echoes exhibit noise due to amplified spontaneous emission, however this noise can be seen as a consequence of the entanglement between the atoms and the output light. With a rephasing pulse one can get an "echo" of the amplified spontaneous emission, leading to light with nonclassical correlations at points separated in time, which is of interest in the context of building wide bandwith quantum repeaters. We also suggest a wideband version of DLCZ protocol based on the same ideas.

PACS numbers: 03.67.-a, 32.80.Qk, 42.50 p

I. INTRODUCTION

In order to extend the range of quantum key distribution, quantum networks and tests of Bell inequalities, a method for efficiently generating entanglement over large distances is required. To achieve this goal a quantum repeater is necessary [1]. Such repeaters are generally based on methods for entangling one light field entangled with another at a later point in time. This has led to increasing interest in quantum memories for light, which in conjunction with pair sources would achieve this. Many impressive experiments have been performed in the area of quantum memories and repeaters. The quantum state of a light field has been stored in a vapour cell with high fidelity, and then measured at a later time [2]. Single photons and squeezed states have been stored and recalled [3, 4, 5], and non-classical interference of the light from distant ensembles has been observed [6]. Entanglement [7] of and teleportation[8] between two distant trapped ions has been achieved using an optical channel, using DLCZ type measurement induced entaglement.

Photon echoes have a long history of use in classical signal processing with light [9, 10]. There are now a number of proposals and experiments [11, 12, 13, 14, 15, 16] related to the development of photon echo based quantum memories. A distinct advantage of echo based techniques is that they are multimode [17].

Current photon echo quantum memory techniques, all involve some modification of the inhomogeneous broadening profile. This imposes limits on the range of suitable materials. It would be much more convenient to use something akin to the standard two pulse echo as a quantum memory which doesn't require such modification.

The paper is arranged in three sections. In Sec. II we present the quantum mechanical Maxwell-Bloch equations for atomic and photonic fields. Then in Sec. III,

as an example of this formalism, we present an analysis of the standard two pulse photon echo and its applicability as a quantum memory. The two pulse echo as a quantum memory has already been investigated by others [18]. We revisit the problem here and show that this protocol fails as a quantum memory due to the strong rephasing pulse, which inverts the medium and causes additional noise on the output photonic fields. Finally in Sec. IV, after exploring the origin of this noise, we propose that this noise can be rephased to lead to time separated, temporally multimode, wide bandwith photon streams with non-classical correlations. So while a standard two pulse echo fails as a quantum memory, rephased amplified spontaneous emission (RASE) can be utilized in the DLCZ protocol [19]. With this modified DLCZ protocol, the inhomogeneous broadening no longer limits the time between the write and read pulses but instead increases the bandwidth of the process. This is of significance to current experiments, were the inhomogeneous broadening is an issue[20, 21, 22, 23, 24].

II. QUANTIZED MAXWELL-BLOCH EQUATIONS

We shall model an inhomogeneously broadened collection of two level atoms interacting with a 1-D field propagating in one direction, with the following quantum Maxwell-Bloch equations:

$$\frac{\partial}{\partial t}\hat{\sigma}_-(z,\Delta,t) = i\Delta\,\hat{\sigma}_-(z,\Delta,t) - i\,\hat{a}(z,t)\,\hat{\sigma}_z(z,\Delta,t) \quad (1)$$

$$\frac{\partial}{\partial t}\hat{\sigma}_z(z,\Delta,t) = i\,\hat{a}(z,t)\,\hat{\sigma}_-(z,\Delta,t)$$
$$- i\,\hat{a}^\dagger(z,t)\,\hat{\sigma}_+(z,\Delta,t) \quad (2)$$

$$\frac{\partial}{\partial z}\hat{a}(z,t) = \frac{i\alpha}{2\pi}\int_{-\infty}^{\infty}\hat{\sigma}_-(z,\Delta,t)\,d\Delta, \quad (3)$$

where $\hat{\sigma}_{+,-,z}$ represent the quantum atomic spin operators, $\hat{a}$ is the quantum optical field operator, α is the
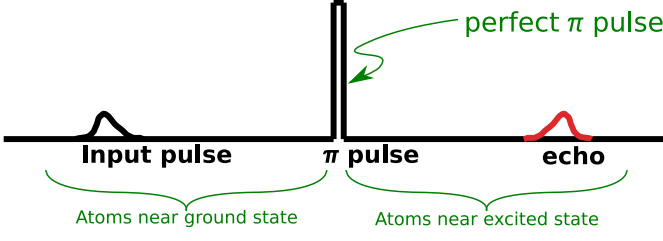
*Electronic address: jevon.longdell@otago.ac.nz

FIG. 1: (Color online) A two pulse photon echo sequence showing the approximations made in the treatment, a weak first pulse is applied to the system and is recalled using and ideal π-pulse.

optical depth parameter, which depends on the coupling between the atoms and the field and on the atom density. The parameter Δ is the detuning from some chosen resonant frequency and z is the distance along the propagation direction. The operators have the following commutation relations:

$$[\hat{a}(z,t), \hat{a}^\dagger(z,t')] = \delta(t - t') \qquad (4)$$
$$[\hat{\sigma}_i(z,\Delta,t), \hat{\sigma}_j(z',\Delta',t)] = \frac{2\pi}{\alpha}\epsilon_{ijk}\hat{\sigma}_k(z,\Delta,t)$$
$$\times \delta(z - z')\delta(\Delta - \Delta') \qquad (5)$$

As can be seen from Eq. 3, we take the density of atoms as a function of frequency to be a constant. In the case of rare earth ion dopants, the inhomogeneous broadening can be many times larger than the homogeneous linewidths, and as a result in most experiments without holeburnt features this is a good approximation.

The above Maxwell-Bloch equations can be derived by dividing the atomic ensemble into thin slices and then modelling each slice as a small collection of atoms inside a Fabry-Perot cavity, using standard input-output theory [25]. Taking the limit as reflectivity of the mirrors go to zero one arrives at Eq. (1–3), where $\hat{a}(z,t)$ is the input field at the left hand side of the cavity and $\hat{a}(z + dz, t)$ is the output field at the right hand side of the cavity.

III. THE TWO PULSE PHOTON ECHO

The first application of our quantum Maxwell-Bloch equations will be in analysing a memory based on a two pulse photon echo. The Maxwell-Bloch equations are non-linear and in general difficult to solve analytically, however following work done with the semiclassical Maxwell-Bloch equations [26] one can make reasonable approximations that simplify the situation greatly. First we shall assume the input pulse is weak and is much smaller than a π pulse. In this case all the atoms will stay near their ground state ($\sigma_z \approx -1$) and we can approximate the atomic lowering operator σ_- as a harmonic oscillator field D_g. The result are linear equations which we shall refer to as the ground state Maxwell-Bloch equations,

$$\frac{\partial}{\partial t}\hat{D}_g(z,\Delta,t) = i\Delta\,\hat{D}_g(z,\Delta,t) + i\,\hat{a}(z,t) \qquad (6)$$
$$\frac{\partial}{\partial z}\hat{a}(z,t) = \frac{i\alpha}{2\pi}\int_{-\infty}^{\infty}\hat{D}_g(z,\Delta,t)\,d\Delta. \qquad (7)$$

Eq. 6 is just a first order linear equation with solution,

$$\hat{D}_g(z,t,\Delta) = -i\int_{-\infty}^{t} dt'\,\hat{a}(z,t')e^{i\Delta(t-t')}$$
$$+ e^{i\Delta t}\hat{D}_{g0}(z,\Delta)\,, \qquad (8)$$

where $\hat{D}_{g0}(z,\Delta)$ is an initial condition. Taking the Fourier transform of Eqs. 7 and 8 and substituting, one arrives at the following expression:

$$\frac{\partial}{\partial z}\hat{a}(z,\omega) = \frac{-\alpha}{2\pi}\int_{-\infty}^{\infty} d\Delta\,\hat{a}(z,\omega)\left[\frac{1}{i(\omega - \Delta)} + \pi\delta(\omega - \Delta)\right]$$
$$+ \frac{i\alpha}{\sqrt{2\pi}}\int_{-\infty}^{\infty} d\Delta\,\delta(\omega - \Delta)\hat{D}_{g0}(z,\Delta)\,,$$
$$= \frac{-\alpha}{2}\hat{a}(z,\omega) + \frac{i\alpha}{\sqrt{2\pi}}\hat{D}_{g0}(z,\omega), \qquad (9)$$

where $\delta(\omega)$ is the Dirac delta function. Solving Eq. 9 and fourier transforming back to the time domain we get

$$\hat{a}(z,t) = \hat{a}(0,t)e^{-\alpha z/2}$$
$$+ \frac{i\alpha}{\sqrt{2\pi}}\int_0^z dz'\,e^{\alpha(z'-z)/2}\,\hat{D}_{g0}(z',t)\,, \qquad (10)$$

where $\hat{a}(0,t)$ denotes the input photonic field. Eqs. 8 and 10 form the ground state solutions for all input times.

After the π-pulse the atoms are all very close to the excited state ($\sigma_z \approx +1$) in which case we can approximate σ_+ by a harmonic oscillator field D_e. This gives us the excited state Maxwell-Bloch equations.

$$\frac{\partial}{\partial t}\hat{D}_e^\dagger(z,\Delta,t) = i\Delta\,\hat{D}_e^\dagger(z,\Delta,t) - i\,\hat{a}(z,t) \qquad (11)$$
$$\frac{\partial}{\partial z}\hat{a}(z,t) = \frac{i\alpha}{2\pi}\int_{-\infty}^{\infty}\hat{D}_e^\dagger(z,\Delta,t)\,d\Delta. \qquad (12)$$

We treat the π pulse as being a perfect π leading to the transformation $\hat{D}_e \leftarrow \hat{D}_g$. We will discuss the treatment of the perfect π pulse later in the text.

Bringing Eqs. 11 and 12 through the same mathematical process as Eqs. 6 and 7, we arrive at the excited state solutions:

$$\hat{D}_e^\dagger(z,t,\Delta) = i\int_{-\infty}^{t} dt'\,\hat{a}(z,t')e^{i\Delta(t-t')} + e^{i\Delta t}\hat{D}_{e0}^\dagger(z,\Delta)\,, \qquad (13)$$

$$\hat{a}(z,t) = \hat{a}(0,t)e^{\alpha z/2}$$
$$+ \frac{i\alpha}{\sqrt{2\pi}} \int_0^z dz'\, e^{\alpha(z-z')/2}\, \hat{D}_{e0}^\dagger(z',t)\,, \quad (14)$$

where $\hat{a}(0,t)$ and $\hat{D}_{e0}^\dagger(z,\Delta)$ are initial conditions for the photonic and atomic excited fields respectively.

Matching the ground (Eqs. 8 and 10) and excited (Eqs. 13 and 14) state solutions at the point the π-pulse is applied we get a complete solution. The efficiency is $\sinh^2(\frac{\alpha z}{2})$ and in the limit of large optical depths high efficiencies are possible. Physically, this is because the photon echo is produced in the first piece of the sample and then gets amplified as it propagates through the inverted medium. The noise on the output can be quantified by considering the case of no input pulse, then the output will be amplified spontaneous emission (ASE), simply the vacuum noise amplified by the gain of $\exp(\alpha z)$ of the inverted ensemble. In the case of no input pulse, we get an incoherent output field with $\langle a^\dagger(t)a(t')\rangle = \delta(t-t')(\exp(\alpha l)-1)$.

It is interesting to consider the source of this noise. In the model we have no dissipation and so the total system evolves through pure states.

Eq. 8 is analogous the output of a beam splitter. The input fields being light and atoms, with the output fields consisting of combinations of photonic and atomic excitations. One can see that the addition of atomic excitations in the solution is necessary for the conservation of the commutation relations due to the input photonic field decaying away at large αl. The excited state solution is analogous to a non-degenerate parametric amplifier [27], here the input field is amplified, and the comutation relations are preserved by the addition of atomic creation operators. The state of one output mode is only mixed if the other is traced over, if the system is viewed as a whole one has an entangled state. In the next section we show that by applying a rephasing pulse to the ensemble we can turn the excitation of the atoms back into light, leading to streams of photons with highly non-classical correlations between two points separated in time.

IV. REPHASED AMPLIFIED SPONTANEOUS EMISSON

Now we consider the two π pulse sequence shown in Fig. 2. For region 1 the atoms will be inverted due to the first π pulse and hence Eqs. (11, 12) will apply. For region 2 the atoms will be near the ground state due to the refocusing π pulse, hence Eqs. (6, 7) describe the dynamics. We take the second π-pulse to occur at $t=0$.

The solution for the light in region 1 is given by Eqs. 8 and 10 and the solution in region 2 is given by Eqs. 13 and 14. For boundary conditions we take the incident field, $\hat{a}(0,t)$, to be in it's vacuum state as we do for the initial condition $D_{e0}(z,\Delta)$. The initial condition for re-
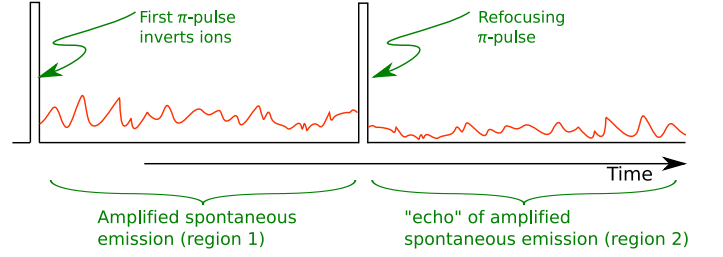

FIG. 2: (Color online) Two π pulse photon echo sequence proposed for generating rephased amplified spontaneous emission (RASE).
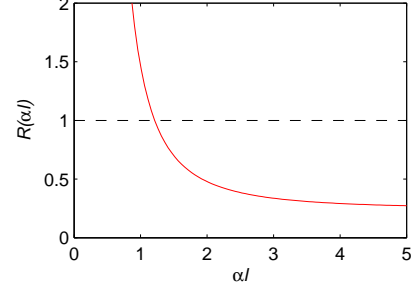

FIG. 3: (Color online) Plot of $R(\alpha l)$, show the violations of the Cauchy-Schwartz inequality for small optical depths.

gion 2 we get from the final condition for region 1:

$$\hat{D}_{g0}(z,\Delta) = ie^{\alpha z/2}\int_{-\infty}^0 dt'\, \hat{a}^\dagger(0,t')\, e^{i\Delta t'}$$
$$+ \frac{\alpha}{\sqrt{2\pi}}\int_{-\infty}^0 dt'\, e^{i\Delta t'}\int_0^z dz'\, e^{\alpha(z-z')/2}\, \hat{D}_{e0}(z',t')$$
$$+ \hat{D}_{e0}(z,\Delta)\,. \quad (15)$$

These boundary and initial conditions substituted in Eqs. (8–14) give a complete analytic solution of the linearised Maxwell-Bloch equations.

To show that the photon streams described by these solutions have non-classical correlations we consider,

$$R \equiv \frac{p(t_1,t_2)^2}{p(t_1,t_1)\,p(t_2,t_2)}, \quad (16)$$

where $p(t_i,t_j) = \langle\, \hat{a}^\dagger(l,t_i)\,\hat{a}(l,t_i)\,\hat{a}^\dagger(l,t_j)\,\hat{a}(l,t_j)\,\rangle$. For classical fields the Cauchy-Schwartz inequality states that $R \leq 1$ [27]. Considering times equally separated about the second π-pulse, from the expression for the output fields derived above we get

$$R(\alpha l) = \left[\frac{1}{2} + \frac{\alpha l + \cosh(\alpha l)}{4\,\sinh\!\left(\frac{\alpha l}{2}\right)\left[e^{\alpha l}-1\right]}\right]^2 \quad (17)$$

Figure 3 shows that for small optical depths ($\alpha l < 1$) the output at times equally separated from the refocusing π-pulse has nonclassical correlations. It should be

pointed out that the entanglement between times is not perfect because the echo efficiency is not 100%. The detection of a photon in Region 2 at a particular time means that there must have been one in Region 1 at the matching time, however the converse is not true.

An advantage that RASE has is it's potential implementation in a larger range of systems. This is in contrast with the implementation of current photon echo quantum memories. Current quantum memory echo techniques use very fine spectral features prepared in the inhomogeneous line, rather than the natural inhomogeneous profile and optical rephasing pulses. Indeed the fact that AFC[15] and CRIB[11, 12] type echoes ideally want homogeneously broadened ensembles, has led to their investigation in non-solid-state systems [28]. When selecting a rare earth ion system, one finds that the systems long lived spectral holes, such as europium or praseodymium, have inconvenient wavelengths ($\approx$ 580 nm and $\approx$ 606 nm), in systems which are much more compatible with optical fibers and diode lasers the holes are much more transient, making high fidelity operation difficult at best.

V. IMPERFECT π PULSES

So far we have treated the π pulses as ideal and the effect of non-ideal π pulses needs to be considered. It is feasible to make a pulse such that afterward one can make the approximation $\sigma_z \approx 1$ especially as we are interested in optically thin samples. The ability to do this in optically thick samples is also helped by the area theorem, which states that a π pulse remains a π pulse as it propagates through a medium [18, 29]. In the situation where $\sigma_z \approx 1$ after the pulse, we can model our non-ideal π pulse as the combination of an ideal π pulse and some excitation of the $\hat{D}_e$ field. This excitation of the $\hat{D}_e$ field will be temporally brief, and if the inhomogeneous broadening is flat the ensemble of atoms will quickly dephase leading to no net polarization in the ensemble shortly after the π pulse. This means that the excitation produced by the imperfect π pulse will no longer interact with the optical field (unless it is rephased by another strong pulse). The ability to prepare an ideal inverted medium for classical information processing has been investigated experimentally [30].

VI. PHASE MATCHING

The treatment so far has involved only one spatial dimension. One way to consider the effect of phase matching is by extending to a 3D treatment in the paraxial approximation. In this case we replace $a(z, t) \rightarrow a(z, \mathbf{k}_t, t)$ and $\sigma_-(z, \Delta, t) \rightarrow \sigma_-(z, \rho, \Delta, t)$ where $\mathbf{k}_t = (k_x, k_y)$ is the transverse wavevector and $\rho = (x, y)$ is the transverse position. Our linearized Maxwell Bloch equations for the ground state become

$$
\begin{aligned}
\frac{\partial}{\partial t} \hat{D}_g(z, \rho, \Delta, t) &= i\Delta \, \hat{D}_g(z, \rho, \Delta, t) \\
&\quad + \frac{i}{4\pi^2} \int d^2 \mathbf{k_t} \, \hat{a}(z, \mathbf{k}_t, t) e^{i\mathbf{k}_t \cdot \rho} \quad (18)
\end{aligned}
$$

$$
\begin{aligned}
\frac{\partial}{\partial z} \hat{a}(z, \mathbf{k}_t, t) &= \\
\frac{i\alpha}{2\pi} \int d^2 \rho \int_{-\infty}^{\infty} d\Delta \quad \hat{D}_g(z, \rho, \Delta, t) e^{-i\mathbf{k}_t \cdot \rho}. \quad (19)
\end{aligned}
$$

Fourier transforming the atomic operators along the transverse dimensions by defining

$$
\hat{D}_g(z, \mathbf{k}_t, \Delta, t) = \int d^2 \rho \, \hat{D}_g(z, \rho, \Delta, t) \exp(-i\mathbf{k}_t . \rho) \quad (20)
$$

leads to Maxwell Bloch equations which are diagonal in the transverse wave vector

$$
\frac{\partial}{\partial t} \hat{D}_g(z, \mathbf{k}_t, \Delta, t) = i\Delta \, \hat{D}_g(z, \mathbf{k}_t, \Delta, t) + i\hat{a}(z, \mathbf{k}_t, t) \quad (21)
$$

$$
\frac{\partial}{\partial z} \hat{a}(z, \mathbf{k}_t, t) = \frac{i\alpha}{2\pi} \int_{-\infty}^{\infty} d\Delta \, \hat{D}_g(z, \mathbf{k}_t \Delta, t). \quad (22)
$$

For the excited state Maxwell Bloch, the same procedure gives

$$
\frac{\partial}{\partial t} \hat{D}_e^\dagger(z, \mathbf{k}_t, \Delta, t) = i\Delta \, \hat{D}_e^\dagger(z, \mathbf{k}_t, \Delta, t) - i \, \hat{a}(z, -\mathbf{k}_t, t) \quad (23)
$$

$$
\frac{\partial}{\partial z} \hat{a}(z, \mathbf{k}_t, t) = \frac{i\alpha}{2\pi} \int_{-\infty}^{\infty} \hat{D}_e^\dagger(z, -\mathbf{k}_t, \Delta, t) \, d\Delta. \quad (24)
$$

In the situation where the π-pulse is applied off axis the phase of the π-pulse depends on the transverse position leading to the transformation

$$
\hat{D}_e(z, \rho, \Delta, t) \leftarrow \hat{D}_g(z, \rho, \Delta, t) \exp(2i\mathbf{k}_\pi . \rho), \quad (25)
$$

or after fourier transforming

$$
\hat{D}_e(z, \mathbf{k}_t, \Delta, t) \leftarrow \hat{D}_g(z, \mathbf{k}_t - 2\mathbf{k}_\pi, \Delta, t). \quad (26)
$$

With the RASE pulse sequence described in Fig. 2, the phase of the first π pulse doesn't matter. The atoms are all in the ground state before the pulse and assuming a perfect π pulse will end up in the excited state afterward regardless. Any small coherent excitation caused by imperfect π pulses can be ignored, it will quickly dephase because of the inhomogeneous broadening and will not be rephased as an echo until after the second π pulse which is outside the region of time of interest. The ASE caused by the inversion due to this π-pulse will be spatially multimode, with the amount of ASE in a particular mode determined by the gain experienced traversing the sample.
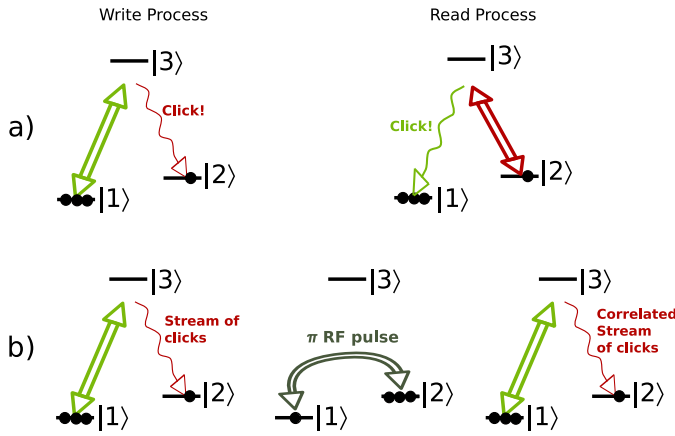
FIG. 4: (Color online) a) DLCZ protocol showing write and read process. b) Modified protocol. The inhomogeneous broadening of the $|1\rangle$-$|2\rangle$ transition now leads to an increase in bandwidth.

Suppose we set a detection system to look at the ASE produced with wavevector $\mathbf{k}_{\mathrm{ASE}}$, from Eqs. 23 and 24. We can see that the light with this wavevector is entangled with the atomic excitation with mode $-\mathbf{k}_{\mathrm{ASE}}$. The π-pulse transfers this to the wavevector $-\mathbf{k}_{\mathrm{ASE}} + 2\mathbf{k}_{\pi}$ according to Eq. 26. Equations 21 and 22 connect atomic and optical modes with the same wavevector so we have that the wavevector for the RASE is $\mathbf{k}_{\mathrm{RASE}} = -\mathbf{k}_{\mathrm{ASE}} + 2\mathbf{k}_{\pi}$ or

$$\mathbf{k}_{\mathrm{ASE}} + \mathbf{k}_{\mathrm{RASE}} = 2\mathbf{k}_{\pi}. \tag{27}$$

This is the same phase matching condition as a two pulse photon echo, $\mathbf{k}_{\mathrm{input}} + \mathbf{k}_{\mathrm{echo}} = 2\mathbf{k}_{\pi}$. While this phase matching condition is valid outside the paraxial regime, the only way to achieve phasematching is with the beams colinear or close to conlinear, because the ASE the RASE and the π pulse must all be at the same frequency.

A. DLCZ

It is interesting to consider the relationship of the current scheme with the DLCZ protocol [19]. The DLCZ protocol involves the creation of entanglement between distant ensembles. The relevant energy level diagrams are shown in Fig. 4a. Once the level $|3\rangle$ has been adiabatically eliminated the write process is formally equivalent

to a set of excited state atoms ($|1\rangle$) spontaneously emitting into the level $|2\rangle$. The emitted optical field is then steered elsewhere for entanglement generation with another ensemble of atoms [19]. Once entanglement is generated between two ensembles, one wishes to read out one ensembles atomic field to a photonic field in order to implement entanglement swapping [19]. For the read process, state $|2\rangle$ becomes the excited state and state $|1\rangle$ the ground state.

One problem with this is the inhomogeneous broadening of the $|1\rangle$-$|2\rangle$ transition causes dephasing limiting the time separation between the writing and reading process. A modified DLCZ protocol, in close analogy with RASE, would overcome this problem. A rephasing pulse on the $|1\rangle$-$|2\rangle$ transition utilizes the inhomogeneous broadening, now increasing the bandwidth of the process rather than reducing the time separations. The sequence of events for this modified DLCZ protocol are shown in Fig. 4b. It is worth noting that the modified DLCZ protocol does not have the same issue with echo efficiency as the two level scheme because the classical coupling field can be altered meaning that the ensemble can be optically thin for the writing process and thicker for the reading process.

The phase matching conditions for the modified DLCZ protocol will be the same as given in Eq. 27 for RASE. However with a Raman transition it is the wavevector difference for the two optical fields that is important. This means that one has alot more freedom in the implementation because one isn't restricted by the requirement that $\omega = ck$, as one is in the two level case.

VII. CONCLUSION

In conclusion we have shown that rephased amplified spontaneous emission has strongly non-classical correlations with the original amplified spontaneous emission in the optically thin regime. This leads to the possibility of a modified DLCZ protocol, where the problem of dephasing due to inhomogeneous broadening of the hyperfine transitions is solved by a rephasing pulse, increasing the bandwidth of the process.

[1] H.-J. Briegel, W. Dür, J. I. Cirac, and P. Zoller, Phys. Rev. Lett. **81**, 5932 (1998).
[2] B. Julsgaard, J. Sherson, J. I. Cirac, J. Fiurasek, and E. S. Polzik, Nature **432**, 482 (2004).
[3] M. D. Eisaman, A. André, F. Massou, M. Fleischhauer, A. S. Zibrov, and M. D. Lukin, Nature **438**, 837 (2005).
[4] T. Chaneliére, D. N. Matsukevich, S. D. Jenkins, S.-Y. Lan, T. A. B. Kennedy, and A. Kuzmich, Nature **428**, 833 (2005).
[5] J. Appel, E. Figueroa, D. Korystov, M. Lobino, and A. I.

Lvovsky, Phys. Rev. Lett. **100**, 093602 (2008).
[6] T. Chanelière, D. N. Matsukevich, S. D. Jenkins, S.-Y. Lan, R. Zhao, T. A. B. Kennedy, and A. Kuzmich, Phys. Rev. Lett. **98**, 113602 (2007).
[7] D. L. Moehring, P. Maunz, S. Olmschenk, K. C. Younge, D. N. Matsukevich, L.-M. Duan, and C. Monroe, Nature **449**, 68 (2007).
[8] S. Olmshenk, D. N. Matsukevich, P. Maunz, D. Hayes, L.-M. Duan, and C. Monroe, Science **323**, 486 (2009).
[9] N. A. Kurnit, I. D. Abella, and S. R. Hartmann, Phys.

Rev. Lett. **13**, 567 (1964).

[10] T. W. Mossberg, Opt. Lett. **7**, 77 (1982).

[11] S. A. Moiseev and S. Kröll, Phys. Rev. Lett. **87**, 173601 (2001).

[12] G. Hétet, J. J. Longdell, A. L. Alexander, P. K. Lam, and M. J. Sellars, Phys. Rev. Lett. **100**, 023601 (2008).

[13] A. L. Alexander, J. J. Longdell, M. J. Sellars, and N. B. Manson, J. Lumin **127**, 94 (2007).

[14] M. U. Staudt, S. R. Hastings-Simon, M. Nilsson, M. Afzelius, V. Scarani, R. Ricken, H. Suche, W. Sohler, W. Tittel, and N. Gisin, *Fidelity of an optical memory based on stimulated photon echoes* (2007).

[15] H. de Riedmatten, M. Afzelius, M. U. Staudt, C. Simon, and N. Gisin, Nature **456**, 773 (2008).

[16] M. Hosseini, B. M. Sparkes, G. Hétet, J. J. Longdell, P. K. Lam, and B. C. Buchler, Nature **461**, 241 (2009).

[17] C. Simon, H. de Riedmatten, M. Afzelius, N. Sangouard, H. Zbinden, and N. Gisin, Phys. Rev. Lett. **98**, 190503 (2007).

[18] J. Ruggiero, J.-L. Le Gouët, C. Simon, and T. Chanelière, Phys. Rev. A **79**, 053851 (2009).

[19] L. M. Duan, M. D. Lukin, J. I. Cirac, and P. Zoller, Nature **414**, 413 (2001).

[20] D. Felinto, C. W. Chou, H. de Riedmatten, S. V. Polyakov, and H. J. Kimble, Phys. Rev. A **72**, 053809 (2005).

[21] J. Laurat, K. S. Choi, H. Deng, C. W. Chou, and H. J. Kimble, Phys. Rev. Lett. **99**, 180504 (2007).

[22] A. Kuzmich, W. P. Bowen, A. D. Boozer, A. Boca, C. W. Chou, L. M. Duan, and H. J. Kimble, Nature **423**, 731 (2003).

[23] C. W. Chou, H. de Riedmatten, D. Felinto, S. V. Polyakov, S. J. van Enk, and H. J. Kimble, Nature **438**, 828 (2005).

[24] H. de Riedmatten, J. Laurat, C. W. Chou, E. W. Schomburg, D. Felinto, and H. J. Kimble, Phys. Rev. Lett. **97**, 113603 (2006).

[25] C. W. Gardiner and M. J. Collett, Phys. Rev. A **31**, 3761 (1985).

[26] L. Tsang, C. S. Cornish, and W. R. Babbitt, J. Opt. Soc. Am. B **20**, 379 (2003).

[27] D. F. Walls and G. J. Milburn, *Quantum Optics* (Springer, 1994).

[28] G. Hétet, M. Hosseini, B. M. Sparks, D. Oblak, P. K. Lam, and B. C. Buchler, Opt. Lett. **33**, 2323 (2008).

[29] E. L. Hahn, N. S. Shiren, and S. L. McCall, Phys. Lett. **37**, 265 (1971).

[30] I. Zafarullah, M. Tian, T. Chang, and W. R. Babbitt, J. Lumin **127**, 158 (2007).